biomedicines

MDPI

Brief Report

Specific Detection of Sialyltransferase ST3GAL3 Towards Lipid Acceptors by Liquid Chromatography Coupled with Tandem Mass Spectrometry Indicates Total Loss of Enzyme Activity in ST3GAL3 Pathogenic Variants

Sara Penati [1], Michele Dei Cas [1], Linda Montavoci [1], Anna Caretti [1] and Marco Trinchera [2,*]

[1] Department of Health Sciences, San Paolo Hospital, Università Degli Studi di Milano, 20142 Milano, Italy; sara.penati@unimi.it (S.P.); michele.deicas@unimi.it (M.D.C.); linda.montavoci@unimi.it (L.M.); anna.caretti@unimi.it (A.C.)

[2] Dipartimento di Medicina e Chirurgia, Università dell'Insubria, via JH Dunant 5, 21100 Varese, Italy

* Correspondence: marco.trinchera@uninsubria.it

Abstract

Background: Pathogenic ST3GAL3 variants cause neurological and cognitive impairment, defining a distinct congenital disorder of glycosylation (ST3GAL3-CDG). Nonetheless, limited enzyme characterization exists due to the lack of a non-radiochemical assay. **Methods**: Here, we developed an LC-MS/MS-based method using the artificial substrate para-nitrophenyl-lacto-N-biose (LNB-pNP; Galβ1,3GlcNAcβ1-O-C6H4NO2) to measure ST3GAL3 activity in vitro. **Results**: A peak corresponding to sialyl-LNB-*p*NP was detected in reactions with homogenate from HEK-293T cells transfected with pCDNA3 ST3GAL3 plasmid, but was virtually absent in mock-transfected cells. A substrate dependence curve provided an apparent Km value for the substrate (0.40 mM) and closely matched values from prior radiochemical methods. No activity was detected with homogenates from cells expressing pathogenic ST3GAL3 variants, except p.A13D, which is known to retain about 10% of residual activity. Compared to ST3GAL4 and ST3GAL6, ST3GAL3 showed markedly higher specificity toward LNB-*p*NP, lactotetraosylceramide (Lc4) and asialo-GM1, which are rather specific substrates. Instead, neo-lactotetraosylceramide (neoLc4) was processed by all three ST3GALs. **Conclusions**: These findings suggest that ST3GAL4 or ST3GAL6 cannot compensate for ST3GAL3 loss in the biosynthesis of gangliosides sialyl-Lc4 and GM1b, but may do so for sialyl-neoLc4. This non-radiochemical assay enables screening and diagnostic evaluation of novel ST3GAL3 variants potentially associated with ST3GAL3-CDG.

Keywords: congenital disorder of glycosylation; ganglioside; glycosphingolipid; sialylation

Academic Editor: Paul Rösch

Received: 23 December 2025
Revised: 26 January 2026
Accepted: 10 February 2026
Published: 12 February 2026

1. Introduction

The *ST3GAL3* gene encodes β-galactoside α2,3-sialyltransferase 3 (ST3GAL3), one of six members of the ST3GALs that transfer sialic acid from CMP-sialic acid to various galactose-containing substrates [1]. ST3GAL3 is a member of the glycosyltransferase family 29 [2] and a Golgi-localized type II membrane protein that can be secreted into body fluids. However, each glycosyltransferase exhibits some peculiarities, such as substrate specificity, discriminating between the sugars, linkages preceding galactose in the glycan chain, or even the aglycone moiety. For instance, ST3GAL5 is the primary ganglioside GM3 and GM4 synthase, acting specifically on lactosylceramide or galactosylceramide [3]. Similarly,

ST3GAL1 and ST3GAL2 prefer chains terminating with the Galβ1,3GalNAc sequence, with ST3GAL1 mainly responsible for mucin biosynthesis and ST3GAL2 for the synthesis of gangliosides GD1a and GT1b [4,5]. ST3GAL3, ST3GAL4 and ST3GAL6 prefer the terminal Galβ1,3/4 sequence, frequently found on N-glycans [6]. In particular, ST3GAL3 primarily acts on saccharides ending with the Galβ1,3GlcNAc sequence, while retaining some activity toward Galβ1,4GlcNAc and on glycosphingolipids with the Galβ1,3GalNAc sequence [7,8]. In contrast, preference for the Galβ1,4GlcNAc ends, on specific N-glycans, has been reported for ST3GAL4 and ST3GAL4 [9,10]. ST3GAL6 also acts on the neolacto-series glycolipids with low and context-dependent efficiency [11].

Pathogenic variants of ST3GAL3 were first identified in 2011 [12] and associated with non-syndromic intellectual disability, thereby defining a novel congenital disorder of glycosylation, ST3GAL3-CDG [13,14]. The ST3GAL3 gene is located on chromosome 1 within the MRT4 locus, previously linked to autosomal recessive non-syndromic intellectual disability (AR-NSID), and represents one of over 200 genes implicated in NSID [15]. In 2020, two siblings carrying a truncated nonsense inactivating ST3GALT3 variant were found to have the same high levels of circulating CA19.9 in their blood as healthy controls, indicating that ST3GAL3 activity is rescued by other ST3GALs in the synthesis of the sialyl-Lewis a tetrasaccharide (Siaα2,3Galβ1,3[Fuca1,4]GlcNAc) epitope on the CA19.9 antigen [8]. Instead, previous studies—using human gastric cancer cell lines—suggested that ST3GAL3 is essential for sialyl-Lewis a synthesis [16].

To date, thirteen ST3GAL3 variants (Supplementary Table S1) have been reported [8,12,17–23], most associated with epileptic encephalopathies.

So far, most ST3GAL3-CDG cases and their cognate ST3GAL3 pathogenic variants have been characterized from clinical and genetic perspectives, with limited functional characterization. Consequently, the biochemical properties of the enzyme and the phenotype–variant relationship remain poorly understood, partly due to the lack of reliable, non-radiochemical assays. To fill this gap, we used the artificial substrate LNB-*p*NP (para-nitrophenyl-lacto-N-biose, Galβ1,3GlcNAcβ1-O-C6H4NO2), previously used in the classic radiochemical assay [8,12], to develop a method based on liquid chromatography coupled with tandem mass spectrometry (LC-MS/MS) to measure ST3GAL3 enzymatic activity in vitro. To our knowledge, LC-MS/MS assays for ST3GAL3 activity have not been reported previously. For other glycosyltransferases, LC-MS/MS has provided more accurate and sensitive measurement than classical radiochemical methods, particularly for low-concentration samples, while also offering enhanced safety and reproducibility [24–26]. We also tested the hypothesized natural substrates of ST3GAL3-Lc4, neoLc4, and asialo-GM1—to assess substrate specificity under near-physiological conditions. Considering the evolutionary proximity within the β-galactoside α2,3-sialyltransferase family, we extended the assay to ST3GAL4 and ST3GAL6 to compare their substrate selectivity and catalytic efficiency towards glycolipid substrates. Moreover, we generated expression plasmids encoding several pathogenic ST3GAL3 variants and assessed their activity in vitro using our novel LC-MS/MS approach.

2. Materials and Methods

2.1. Sialyltransferase Activity Assay

LNB-*p*NP (Tokyo Chemical Industry, Tokyo, Japan, G0420), used as a sialyltransferase acceptor in amounts from 0.125 to 30 nmol per assay, was dissolved in chloroform/methanol, 1:1 (*v*/*v*) together with 20 µg Triton-X100, and placed at the bottom of 0.6 mL microcentrifuge tubes. They were allowed to dry at RT under a hood, and then kept at −20 °C until used. A reaction solution was prepared and added to each tube to obtain the following final concentrations: 0.2 M Tris/HCl pH 7.0 and 2.5 mM CMP-sialic acid (Sigma

Aldrich, St Louis, MA, USA). In an ice-bucket, 1.0–100 μg of homogenate protein was added to each tube already containing water to a final volume of 20 μL. The reactions were started by placing the tubes at 37 °C and incubating them for 60 min, and the reactions were stopped by placing the tubes on ice and then storing them at −20 °C. As sialyl-LNB-pNP is not commercially available, it was synthesized for mass spectrometry analysis via a quantitative conversion (24 h at 37°, 94%) of LNB-pNP (4 nmol), employing the homogenate of ST3GAL3-transfected HEK-293T cells as the enzymatic source. Sialyltransferase activity assay was also performed using natural sphingolipid acceptors such as asialo-GM1, prepared as reported [8], nLc4 and Lc4 (C18:0 Lc4 Ceramide, Avanti Polar, Alabaster, AL, USA). nLc4 was obtained by neuraminidase treatment (α2-3,6,8 neuraminidase, P0720S, New England Biolabs, Ipswich, MA, USA) of sialyl neolactotetraosylceramide (snLc4, Neu5Acα(2-3)Galβ(1-4)GlcNAcβ(1-3)Galβ(1-4)Glc-18:0 ceramide, S0910, TCI Chemicals Europe, Zwijndrecht, Belgium), incubating 100 μg of snLc4 with 1 μL of neuraminidase (50 U) in 10 μL of 1x glycobuffer 1 (New England Biolabs) for 4h at 37 °C and then for an additional 4h after adding 1 μL of fresh neuraminidase. The reaction rate—monitored by HR-MS (Lc4 d18:1/18:0, $[MH]^{2+}$ 628.3979)—after the first and second incubation was 70% and >95%, respectively. One nmol of asialo-GM1, and 0.15 nmoles of both nLc4 and Lc4, were used as acceptors in the assay after mixing with 20 μg of Triton-X100, as for LNB-*p*NP. The reaction mixture and incubation were as for LNB-*p*NP, but in a final volume of 10 μL. GM1a was purchased from Avanti Polar (Alabaster, AL, USA) and GM1b was kindly provided by Prof. Roger Sandhoff, who isolated the ganglioside from the brain of a ST3GAL5-KO mouse. For apparent kinetic constant calculations, the Hanes–Woolf plot was used. The curves were obtained at fixed CMP-Sial concentration (2.5 mM) and varying substrate LNB-*p*NP concentration from 0 to 3.0 mM. The reactions were performed by incubating 20 μg of homogenate protein from ST3GAL3-transfected HEK-293T cells, 40 μg from ST3GAL4, and 90 μg from ST3GAL6 transfections for 60 min, which assured initial rates. Vmax values were calculated starting from specific activity values expressed as nmoles of sialyl-LNB-*p*NP formed by 1.0 mg of homogenate protein per hour of incubation.

2.2. Reaction Product Characterization and Quantification by LC-MS/MS

For assaying sialyltransferase activity, reactions were precipitated by addition of pure acetonitrile (80 μL) and centrifugated at 11,400 rpm for 10 min. The precipitates were discharged, and pure extracts were diluted with water (1:1, *v*/*v*) and directly injected into LC-MS/MS. The LC-MS/MS apparatus consisted of a LC Dionex 3000 UltiMate (ThermoFisher Scientific, Waltham, MA, USA) coupled to a tandem mass spectrometer AB Sciex 3200 QTRAP (AB Sciex, Concord, ON, Canada) equipped with an electrospray ionization TurboIonSpray™ source operating in positive mode (ESI+). Chromatographic separation was carried out on a reverse-phase Cortecs T3 column with 2.7 μm particle size, 100 × 2.1 mm (Waters, Franklin, MA, USA), using a linear gradient elution with two solvents: 0.1% formic acid and 5 mM ammonium formate in water (solvent A) and acetonitrile (solvent B). The flow rate was set at 0.25 mL/min, the temperature at 35 °C and the injection volume at 3 μL. The elution gradient (%B) was set as follows: 0–2 min (5%), 2–11 min (5–90%), 11–12 min (90%), and 12–12.2 min (90–5%), held until 15 min. The analytes were monitored by multiple reaction monitoring as follows: the substrate LNB-p-NP ($[MH]^+$ 505.5 > 138, DP 25, CE 25 eV) and the sialylated product sialyl-LNB-p-NP ($[MH]^+$ 796.25 > 138, DP 25, CE 25 eV). Confirmatory ions were monitored as well: for LNB-p-NP *m/z* 204 and for sLNB-p-NP *m/z* 204, 292. High-resolution mass spectra with structural elucidation of LNB-pNP and sialyl-LNB-pNP can be found in Supplementary Figure S1. The extracts—obtained by methanol (90 μL) precipitation—from the reactions with natural sphingolipids were analyzed using an Acquity BEH C18 column with 1.7 μm particle size,

50 × 2.1 mm (Waters, Franklin, MA, USA), at 30 °C using a linear gradient elution with two solvents: 0.2% formic acid and 2 mM ammonium formate in water (solvent A) and 0.2% formic acid and 1 mM ammonium formate in methanol (solvent B). The flow rate was set at 0.3 mL/min, the temperature at 30 °C and the injection volume at 5 µL. The elution gradient (%B) was set as follows: 0–3 min (80–90%), 3.0–6.0 min (90%), 6.0–19.0 min (90–99%), and 19.0–20.0 min (99–80%), held until 24 min. The analytes were monitored by multiple reaction monitoring as follows: aGM1/Lc4/nLc4 d18:1/18:0 ($[MH]^{2+}$ 628.39 > 264.3, DP 60, CE 40 eV) and GM1b/sLc4/snLc4/GM1a d18:1/18:0 ($[MH]^{2+}$ 773.94> 264.3, DP 60, CE 50 eV).

3. Results and Discussion

ST3GAL activity has been previously measured in vitro using a radiochemical assay with radioactive CMP-sialic acid and various acceptors, including oligosaccharides and LNB-*p*NP. Leveraging the efficient ionization of the *p*NP moiety, we developed an LC–MS/MS method to detect ST3GAL3 activity toward LNB-*p*NP using non-radioactive CMP-sialic acid, quantifying the sialyl-LNB-*p*NP product. Under established reaction conditions, a distinct sialyl-LNB-*p*NP peak was observed with the homogenate from HEK-293T cells transfected with pCDNA3 ST3GAL3 plasmid (Figure 1A), whereas mock-transfected cells showed no peak above baseline (<20 pmol). To validate ST3GAL3 activity measurement, we generated a substrate saturation curve, providing an apparent Km value for the substrate (0.4 mM, see Table 1), closely matching values from the radiochemical assay [8].

Table 1. Apparent kinetic constants of ST3GAL3-4-6 toward LNB-*p*NP.

	Km (mM)	Vmax (nmol × mg^{-1} Protein × h^{-1})	Catalytic Efficiency (Vmax/Km)
ST3GAL3	0.40	95.63	239.07
ST3GAL4	19.8	26.90	1.35
ST3GAL6	26	52.14	2.00

The same analytical approach was used to compare the enzymatic activity of ST3GAL3 toward LNB-*p*NP with that of ST3GAL4 and ST3GAL6 (Figure 1A), two sialyltransferases sharing 35.6% and 32.3% sequence identity with ST3GAL3, respectively. In this analysis, ST3GAL3 showed a markedly higher efficiency in converting LNB-*p*NP into sialyl-LNB-*p*NP, reaching a Vmax/Km ratio of 239. In contrast, ST3GAL4 and ST3GAL6 were approximately one hundred times less efficient, with ratios of 1.35 and 2.00, respectively (Table 1). Altogether, these results indicate that LNB-*p*NP is a highly specific substrate for ST3GAL3, supporting the previously proposed preference of this enzyme for glycosphingolipid substrates [8].

The LC–MS/MS assay demonstrated robust performance, suitable for quantifying LNB-pNP and sialyl-LNB-pNP in cellular homogenate. Linearity was confirmed through independent calibration curves over the 0.25–15 nmol range (R^2 > 0.99) for both analytes, using matrix-matched samples derived from enzymatic reactions on mock cell lysates. Limits of detection (LOD) and quantification (LOQ) were determined based on signal-to-noise ratios of 3:1 and 10:1, respectively. The resulting LOD values were 0.05 nmol (LNB-pNP) and 0.12 nmol (sialyl-LNB-pNP), while LOQ values were 0.22 nmol and 0.25 nmol, respectively. Inter- and intra-assay precision, assessed using independent quality control samples (low and medium-high concentrations prepared in lysate matrix, n = 6), showed mean coefficients of variation (CV%) of 4.3–4.1% for LNB-pNP and 9.3–6.6% for sialyl-LNB-pNP. All values were within the acceptable limits (<15–20%) defined by FDA bioanalytical guidelines. Accuracy, determined from the same quality control samples, showed mean recoveries of 110% for LNB-pNP and 100% for sialyl-LNB-pNP (acceptable range: 85–115%

per FDA bioanalytical guidelines). Collectively, these validation parameters confirm the superiority of this assay over traditional radiochemical methods, which are limited by radiolabel instability and lack of multiplexing. Detailed validation data are provided in Supplementary Table S2.

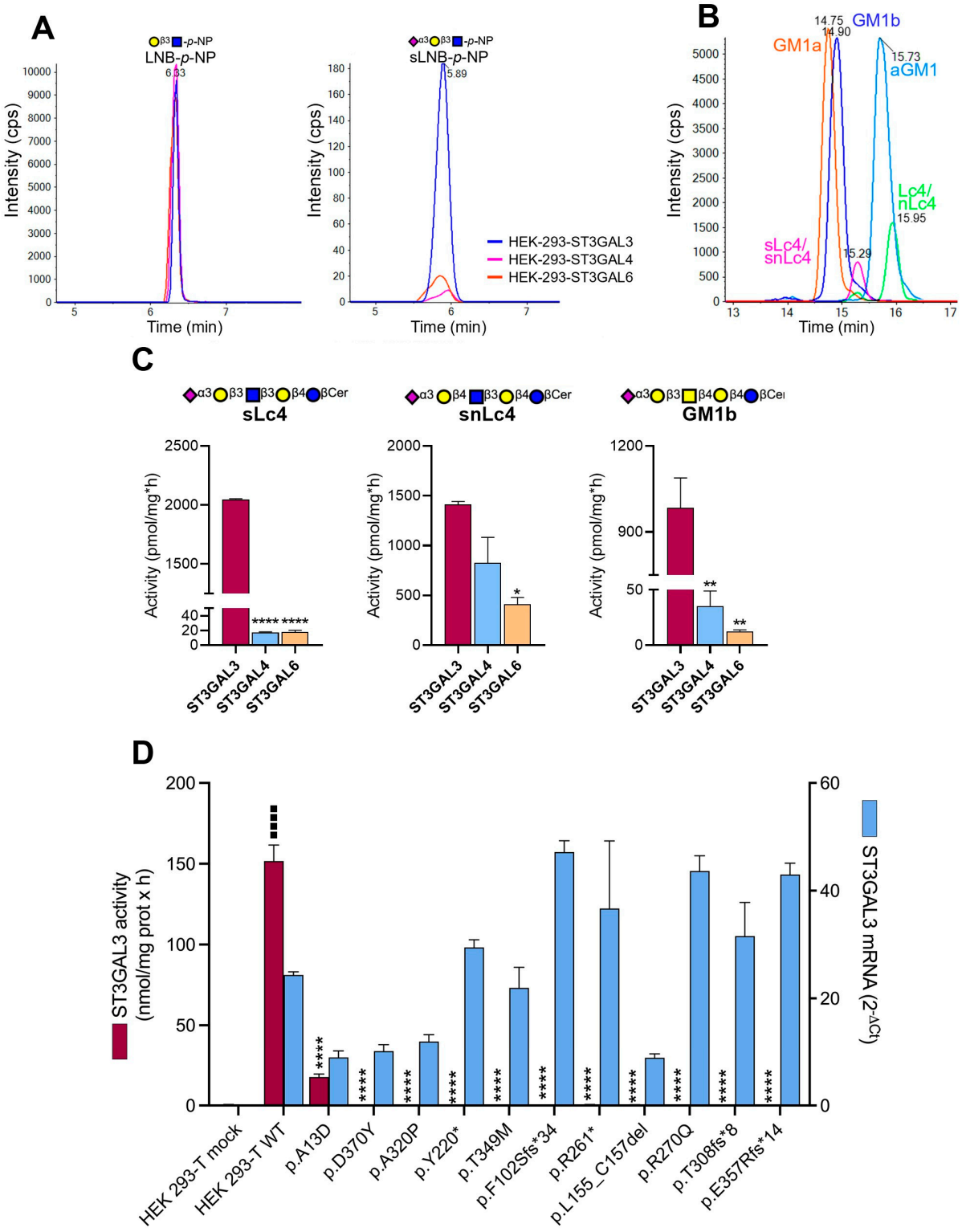

Figure 1. Detection by LC-MS/MS of sialyltransferase activity towards LNB-*p*NP or natural glycosphingolipid substrates. (**A**) Chromatograms of acceptor substrates and sialylated products. Homogenates from HEK-293T cells transfected with WT ST3GAL3/4/6 placed in an expression vector were used as the enzyme source for determining sialyltransferase activity towards LNB-*p*NP.

Left chromatogram: detection of LNB-*p*NP alone; right chromatogram: detection of sialyl-LNB-*p*NP obtained upon incubation with the different enzyme sources. (**B**) Detection of the following natural reference glycosphingolipids: aGM1 (Rt 15.73) > GM1b (14.90); Lc4 (15.95) > sLc4 (15.29); and nLc4 (15.95) > snLc4 (15.29). GM1a (Rt 14.75) is shown underlining the separation from linear isomers such as GM1b and sLc4/snLc4 (unresolved). (**C**) Specific sialytransferase activity measured with ST3GAL3/4/6 towards different acceptors. The same homogenates (10–45 μg) as in panel A were incubated with LNB-*p*-NP (10 nmol, 20 μL final volume), Lc4 or nLc4 (0.15 nmol, 10 μL final volume), or aGM1 (1.0 nmol, 10 μL final volume). The reactions were carried out for 1h at 37 °C and the sialylated products assayed by LC-MS/MS. Significance: * ($p < 0.1$), ** ($p < 0.01$), **** ($p < 0.0001$). (**D**) Sialyltransferase activity of ST3GAL3 variants toward LNB-*p*NP. Homogenates from HEK-293T cells transfected with WT or variant ST3GAL3 were used (up to 100 μg) for determining sialyltransferase activity toward LNB-*p*NP as in panel A. The reaction product sialyl-LNB-*p*NP was assayed by LC-MS/MS. Values are the mean for two independent assays performed in duplicate and are presented after subtracting those obtained using mock-transfected HEK-293T cells as the enzyme source in the reaction. Cell lysates obtained from an aliquot of the same transfections were used for extracting total RNA that was reverse-transcribed and the obtained cDNA submitted to quantitative PCR using primer specific to ST3GAL3 and GAPDH as a reference. The amounts of ST3GAL3 transcript were calculated as $2^{-\Delta Ct}$. Statistical significance was investigated using one-way ANOVA coupled to Bonferroni post hoc test: ■■■■ indicate the significance toward mock-transfected HEK-293T ($p < 0.0001$)], **** indicate the significance toward HEK-293T WT ($p < 0.0001$)]. Variants are defined according to NCBI Reference Sequence NM_006279.5.

To validate the results obtained with the artificial substrate reflected the enzyme natural behavior, three endogenous glycosphingolipids (Lc4, neoLc4, and asialo-GM1) were tested as substrates—under the same reaction conditions—and analyzed by LC–MS/MS. ST3GAL3 exhibited the highest specific activity toward all three substrates (Figure 1B). With Lc4, ST3GAL3 activity exceeded that of ST3GAL4 and ST3GAL6 by more than 100-fold. With asialo-GM1, it was over 30-fold higher than both, whereas with neoLc4, it was approximately threefold higher than ST3GAL6 and not significantly different from ST3GAL4. These results may suggest that glycosphingolipids terminating with a galactose β1,3 linked to an N-acetylhexosamine represent optimal substrates for ST3GAL3 activity in vitro.

Plasmid DNAs, encoding several pathogenic ST3GAL3 variants, were generated by site-directed mutagenesis and transfected into HEK-293T cells. The resulting lysates were used to assess ST3GAL3 transcript expression by RT-qPCR and the cellular homogenates served as a source for enzyme activity performed by LC-MS/MS. All variants displayed high transcript levels comparable to those of WT ST3GAL3. However, no detectable enzymatic activity was observed above the baseline level measured in mock-transfected cells, with the exception of the p.A13D variant, which retained approximately 10% residual activity (Figure 1C). These findings confirm and extend previous reports describing the loss of catalytic function in some pathogenic ST3GAL3 variants [8,12]. Remarkably, the patient carrying the p.A13D variant is the only one reported to present non-syndromic intellectual disability, while the others display an epileptic phenotype. A protective role of the minimal residual activty, against the more severe neurological presentation, can therefore be hypothesized and deserves validation through the analysis of additional patients. As in other CDG, the physiological substrates of ST3GAL3 remain unidentified, as do the specific reaction product(s) that are lost due to the enzyme inactivity.

At present, it remains unclear if the loss of activity of the variants arises from defective protein translation or maturation, protein instability, or defective catalytic function, an aspect that deserves attention in the future. Current evidence points to the possibility that the absence of specific gangliosides may contribute to disease pathogenesis [13,14]. Dedicated studies, aimed at characterizing the glycoconjugate composition and sialylation profile of patient-derived cells, may help clarify this relevant aspect. Overall, the reported

LC-MS/MS approach provides a valuable tool for screening and aiding the diagnosis of novel ST3GAL3 variants potentially associated with ST3GAL3-CDG.

Supplementary Materials: The following supporting information can be downloaded at: https://www.mdpi.com/article/10.3390/biomedicines14020419/s1 [8,26], Supplementary Methods, Figure S1: Mass spectra of LNB-pNP (blue, RT 3.75) and sialyl-LNB-pNP (magenta, RT 3.69) acquired in positive ESI mode on a SCIEX X500B QTOF system, Table S1: List of ST3GAL3 variants reported to date; Table S2: LC-MS/MS method validation, Table S3: Oligonucleotides used in this study.

Author Contributions: Conceptualization, M.D.C. and M.T.; methodology, S.P., L.M., M.D.C. and M.T.; software, L.M.; validation, S.P., L.M., M.D.C. and M.T.; formal analysis, S.P., L.M., M.D.C. and M.T.; investigation, S.P., L.M., M.D.C. and M.T.; writing—original draft preparation, S.P. and M.D.C.; writing—review and editing, M.T. and A.C.; visualization, S.P., L.M. and M.D.C.; and supervision, M.T. All authors have read and agreed to the published version of the manuscript.

Funding: This research was funded by Universita dell'Insubria, Fondo Ateneo Ricerca 2024–2025 (to M.T.) and the PhD program in Translational Medicine of the University of Milan (to S.P.).

Data Availability Statement: Data supporting reported results are available upon request.

Conflicts of Interest: The authors declare no conflicts of interest.

Abbreviations

The following abbreviations are used in this manuscript: LC-MS/MS, liquid chromatography-tandem mass spectrometry. Sialyltransferases are named according to the HUGO recommendations; asialo-GM1, gangliotetraosylceramide, Galβ1,3GalNAcβ1,4Galβ1,4Glc-Cer; Lc4, lactotetraosylceramide, Galβ1,3GlcNAcβ1,3Galβ1,4Glc-Cer; nLc4, neo-lactotetraosylceramide, Galβ1,4GlcNAcβ1,3Galβ1,4Glc-Cer; LNB-*p*NP, *para*-nitrophenyllacto-N-biose, Galβ1,3GlcNAcβ1-O-C6H4NO2; WT, wild-type; RT-qPCR, reverse-transcription quantitative polymerase chain reaction.

References

1. Mohamed, K.A.; Kruf, S.; Büll, C. Putting a cap on the glycome: Dissecting human sialyltransferase functions. *Carbohydr. Res.* **2024**, *544*, 109242. [CrossRef]
2. Harduin-Lepers, A. The vertebrate sialylation machinery: Structure-function and molecular evolution of GT-29 sialyltransferases. *Glycoconj. J.* **2023**, *40*, 473–492. [CrossRef] [PubMed]
3. Uemura, S.; Go, S.; Shishido, F.; Inokuchi, J. Expression machinery of GM4: The excess amounts of GM3/GM4S synthase (ST3GAL5) are necessary for GM4 synthesis in mammalian cells. *Glycoconj. J.* **2014**, *31*, 101–108. [CrossRef]
4. Zhang, N.; Lin, S.; Cui, W.; Newman, P.J. Overlapping and unique substrate specificities of ST3GAL1 and 2 during hematopoietic and megakaryocytic differentiation. *Blood Adv.* **2022**, *6*, 3945–3955. [CrossRef]
5. Blažetić, S.; Krajina, V.; Labak, I.; Viljetić, B.; Pavić, V.; Ivić, V.; Balog, M.; Schnaar, R.L.; Heffer, M. Sialyltransferase Mutations Alter the Expression of Calcium-Binding Interneurons in Mice Neocortex, Hippocampus and Striatum. *Int. J. Mol. Sci.* **2023**, *24*, 17218. [CrossRef] [PubMed]
6. Gu, J.; Isaji, T. Specific sialylation of N-glycans and its novel regulatory mechanism. *Glycoconj. J.* **2024**, *41*, 175–183. [CrossRef]
7. Sturgill, E.R.; Aoki, K.; Lopez, P.H.; Colacurcio, D.; Vajn, K.; Lorenzini, I.; Majic, S.; Yang, W.H.; Heffer, M.; Tiemeyer, M.; et al. Biosynthesis of the major brain gangliosides GD1a and GT1b. *Glycobiology* **2012**, *22*, 1289–1301. [CrossRef]
8. Indellicato, R.; Domenighini, R.; Malagolini, N.; Cereda, A.; Mamoli, D.; Pezzani, L.; Iascone, M.; Dall'olio, F.; Trinchera, M. A novel nonsense and inactivating variant of ST3GAL3 in two infant siblings suffering severe epilepsy and expressing circulating CA19.9. *Glycobiology* **2020**, *30*, 95–104. [CrossRef] [PubMed]
9. Costa, A.F.; Senra, E.; Faria-Ramos, I.; Teixeira, A.; Morais, J.; Pacheco, M.; Reis, C.A.; Gomes, C. ST3GalIV drives SLeX biosynthesis in gastrointestinal cancer cells and associates with cancer cell motility. *Glycoconj. J.* **2023**, *40*, 421–433. [CrossRef]
10. Qi, F.; Isaji, T.; Duan, C.; Yang, J.; Wang, Y.; Fukuda, T.; Gu, J. ST3GAL3, ST3GAL4, and ST3GAL6 differ in their regulation of biological functions via the specificities for the alpha2,3-sialylation of target proteins. *FASEB J.* **2020**, *34*, 881–897. [CrossRef]
11. Ogasawara, N.; Katagiri, Y.U.; Kiyokawa, N.; Kaneko, T.; Sato, B.; Nakajima, H.; Miyagawa, Y.; Kushi, Y.; Ishida, H.; Kiso, M.; et al. Accelerated biosynthesis of neolacto-series glycosphingolipids in differentiated mouse embryonal carcinoma F9 cells detected by using dodecyl N-acetylglucosaminide as a saccharide primer. *J. Biochem.* **2011**, *149*, 321–330. [CrossRef]

12. Hu, H.; Eggers, K.; Chen, W.; Garshasbi, M.; Motazacker, M.M.; Wrogemann, K.; Kahrizi, K.; Tzschach, A.; Hosseini, M.; Bahman, I.; et al. ST3GAL3 mutations impair the development of higher cognitive functions. *Am. J. Hum. Genet.* **2011**, *89*, 407–414. [CrossRef]
13. Inamori, K.I.; Inokuchi, J.I. When ganglioside pathways go awry: Congenital disorders and experimental insights. *J. Hum. Genet.* **2025**, *142*. [CrossRef]
14. Jáñez Pedrayes, A.; Rymen, D.; Ghesquière, B.; Witters, P. Glycosphingolipids in congenital disorders of glycosylation (CDG). *Mol. Genet. Metab.* **2024**, *142*, 108434. [CrossRef] [PubMed]
15. Rivero, O.; Alhama-Riba, J.; Ku, H.P.; Fischer, M.; Ortega, G.; Álmos, P.; Diouf, D.; van den Hove, D.; Lesch, K.P. Haploinsufficiency of the Attention-Deficit/Hyperactivity Disorder Risk Gene St3gal3 in Mice Causes Alterations in Cognition and Expression of Genes Involved in Myelination and Sialylation. *Front. Genet.* **2021**, *12*, 688488. [CrossRef]
16. Carvalho, A.S.; Harduin-Lepers, A.; Magalhães, A.; Machado, E.; Mendes, N.; Costa, L.T.; Matthiesen, R.; Almeida, R.; Costa, J.; Reis, C.A. Differential expression of alpha-2,3-sialyltransferases and alpha-1,3/4-fucosyltransferases regulates the levels of sialyl Lewis a and sialyl Lewis x in gastrointestinal carcinoma cells. *Int. J. Biochem. Cell Biol.* **2010**, *42*, 80–89. [CrossRef]
17. Mahdiannasser, M.; Rashidi-Nezhad, A.; Badv, R.S.; Akrami, S.M. Exploring the genetic etiology of drug-resistant epilepsy: Incorporation of exome sequencing into practice. *Acta Neurol. Belg.* **2022**, *122*, 1457–1468. [CrossRef] [PubMed]
18. Manoochehri, J.; Khamirani, H.J.; Kamal, N.; Shiri, A.; Aghasipour, M.; Hassanipour, H.; Zoghi, S.; Dianatpour, M.; Dastgheib, S.A.; Tabei, S.M.B. ST3GAL3 deficiency with autistic behavior: First description of frameshift variant and literature review. *Gene Rep.* **2024**, *35*, 101892. [CrossRef]
19. Whitney, R.; Jain, P.; RamachandranNair, R.; Jones, K.C.; Kiani, H.; Tarnopolsky, M.; Meaney, B. The epilepsy phenotype of ST3GAL3-related developmental and epileptic encephalopathy. *Epilepsia Open* **2023**, *8*, 623–632. [CrossRef]
20. Farajollahi, Z.; Razmara, E.; Heidari, E.; Jafarinia, E.; Garshasbi, M. A novel variant of ST3GAL3 causes non-syndromic autosomal recessive intellectual disability in Iranian patients. *J. Gene Med.* **2020**, *22*, e3253. [CrossRef]
21. Edvardson, S.; Baumann, A.M.; Muhlenhoff, M.; Stephan, O.; Kuss, A.W.; Shaag, A.; He, L.; Zenvirt, S.; Tanzi, R.; Gerardy-Schahn, R.; et al. West syndrome caused by ST3Gal-III deficiency. *Epilepsia* **2013**, *54*, e24–e27. [CrossRef] [PubMed]
22. Khamirani, H.J.; Zoghi, S.; Faghihi, F.; Dastgheib, S.A.; Hassanipour, H.; Bagher Tabei, S.M.; Mohammadi, S.; Masoudi, M.; Poorang, S.; Ehsani, E.; et al. Phenotype of ST3GAL3 deficient patients: A case and review of the literature. *Eur. J. Med. Genet.* **2021**, *64*, 104250. [CrossRef] [PubMed]
23. Hu, J.; Liu, J.; Guo, C.; Duan, Y.; Liu, C.; Tan, Y.; Pan, Y. Clinical report and genetic analysis of a Chinese patient with developmental and epileptic encephalopathy associated with novel biallelic variants in the ST3GAL3 gene. *Mol. Genet. Genomic Med.* **2024**, *12*, e2322. [CrossRef]
24. Dei Cas, M.; Montavoci, L.; Casati, S.; Malagolini, N.; Dall'Olio, F.; Trinchera, M. Convenient and Sensitive Measurement of Lactosylceramide Synthase Activity Using Deuterated Glucosylceramide and Mass Spectrometry. *Int. J. Mol. Sci.* **2023**, *24*, 5291. [CrossRef]
25. Dei Cas, M.; Casati, S.; Roda, G.; Sardi, P.; Paroni, R.; Fonzo, A.; Trinchera, M. A sensitive method for determining UDP-glucose: Ceramide glucosyltransferase (UGCG) activity in biological samples using deuterated glucosylceramide as acceptor substrate. *Glycobiology* **2022**, *33*, 88–94. [CrossRef]
26. Dei Cas, M.; Montavoci, L.; Pasini, C.; Caretti, A.; Penati, S.; Martinelli, C.; Gianelli, U.; Casati, S.; Nardecchia, F.; Torella, A.; et al. Loss of function and reduced levels of sphingolipid desaturase DEGS1 variants are both relevant in disease mechanism. *J. Lipid Res.* **2024**, *65*, 100517. [CrossRef] [PubMed]